Cancer Cell
Article

Targeted Deletion of the Calcineurin Inhibitor DSCR1 Suppresses Tumor Growth

Sandra Ryeom,[1,*] Kwan-Hyuck Baek,[1] Matthew J. Rioth,[1] Ryan C. Lynch,[1] Alexander Zaslavsky,[1] Amy Birsner,[1] Sam S. Yoon,[2] and Frank McKeon[3]
[1]Vascular Biology Program, Department of Surgery, Children's Hospital, Boston, MA 02115, USA
[2]Division of Surgical Oncology, Department of Surgery, Massachusetts General Hospital, Boston, MA 02114, USA
[3]Department of Cell Biology, Harvard Medical School, Boston, MA 02115, USA
*Correspondence: sandra.ryeom@childrens.harvard.edu
DOI 10.1016/j.ccr.2008.02.018

SUMMARY

The NF-AT transcription factors regulated by the phosphatase calcineurin play a role in breast cancer metastasis-promoting tumor cell invasion. Metastasis is a multistep process requiring angiogenesis and endothelial activation. NF-AT is also expressed in endothelial cells, and calcineurin-NF-AT signaling is an important downstream effector of the proangiogenic cytokine VEGF. One isoform of the endogenous calcineurin regulator, Down syndrome candidate region-1 (DSCR1.Ex4), suppresses calcineurin-NFAT signaling blocking endothelial proliferation. However, overexpression of the other DSCR1 isoform (DSCR1.Ex1) may promote angiogenesis. We report that targeted deletion of both isoforms leads to hyperactivated calcineurin and precocious endothelial apoptosis, inhibiting formation of an effective tumor vasculature and suppressing tumorigenesis. Treatment with the specific pharmacological calcineurin inhibitor cyclosporin A rescues this endothelial defect in *DSCR1*$^{-/-}$ mice, restoring tumor growth.

INTRODUCTION

Oncogenic mutations are thought to be causally involved in the genesis, progression and maintenance of human cancers (Folkman and Ryeom, 2005). Nonetheless, it is also well accepted that tumor evolution, invasion, and metastasis involve obligate and complex interactions between cancer cells and their surrounding host microenvironment (Folkman and Ryeom, 2005). In particular, macroscopic growth of tumor masses requires not only tumor cell proliferation but also concomitant angiogenesis, for which endothelial cell activation is a prerequisite (Folkman and Ryeom, 2005). Endothelial cell activation and proliferation is regulated by multiple proangiogenic factors, of which the most widely studied is vascular endothelial growth factor (VEGF). VEGF is a potent endothelial cell mitogen in vivo (Ferrara, 2004) whose function is critical for angiogenesis in both normal development and adult remodeling tissues as well as in tumor cell expansion and invasion (Ferrara, 2004).

Of the many downstream effectors of VEGF function in endothelial cells, one is the calcineurin-NFAT signaling pathway. Following VEGF ligation of its receptors VEGFR1 and VEGFR2, PLCγ is activated with subsequent increases in intracellular calcium levels (Ferrara et al., 2003). Increased calcium activates the serine/threonine phosphatase calcineurin, which, in turn, dephosphorylates the NF-AT family of transcription factors and triggers their nuclear accumulation (Crabtree and Olson, 2002). NF-AT transactivates multiple proangiogenic genes, such as those encoding cyclooxygenase 2, E-selectin, and tissue factor (Hernandez et al., 2001; Johnson et al., 2003).

The endogenous calcineurin inhibitor Down syndrome candidate region-1 (DSCR1), also known as RCAN1, has two differentially regulated isoforms (Rothermel et al., 2003). Overexpression of the inducible isoform, DSCR1.Ex4, blocks VEGF-calcineurin-NF-AT-mediated activation of endothelial cells in vitro (Hesser et al., 2004; Iizuka et al., 2004; Minami et al., 2004; Yao and Duh, 2004). In contrast, overexpression of

SIGNIFICANCE

Recent anticancer therapies target endothelial cells to block tumor vascularization. Endothelial proliferation is mediated by cytokines like VEGF that activate the endothelium via their cell surface receptors. Antiangiogenic therapy has focused on preventing endothelial activation by sequestering angiogenic factors or targeting their receptors. Here we show that angiogenesis may be regulated in an endothelial cell-autonomous manner downstream of VEGF via modulation of calcineurin signaling. The calcineurin inhibitor DSCR1 attenuates VEGF-calcineurin-NF-AT signaling in endothelial cells. Upon loss of DSCR1, VEGF-calcineurin signaling is hyperactivated, leading to premature endothelial apoptosis and, ultimately, suppression of tumor angiogenesis. Our data illustrate that strict regulation of calcineurin activity in endothelial cells is required for tumor angiogenesis. Thus, the calcineurin pathway represents a tractable target for suppressing tumor growth.

the constitutive isoform DSCR1.Ex1 promotes angiogenesis in vitro (Qin et al., 2006). Hence, the overall influence of the *DSCR1* gene on VEGF-calcineurin-NF-AT-mediated activation of endothelial cells in particular, and on normal and tumor vascular endothelium in general, remains unclear. However, a microarray study looking at gene transcription following VEGF treatment of endothelial cells found *DSCR1.Ex4* to be the most highly upregulated transcript, consistent with an important role for DSCR1 in VEGF-mediated angiogenesis (Abe and Sato, 2001). Recently, a role for the calcineurin substrate NF-AT in cancer progression has been identified. Most notably, NF-AT is expressed in breast cancer cells, where it mediates cancer cell invasion and metastasis as a consequence of downregulation of AKT (Jauliac et al., 2002). Such observations suggest that the calcineurin-NFAT pathway plays a significant role in tumor growth through its actions in cancer cells. However, the extent to which DSCR1 regulates NF-AT activity in cancer cells, either independently or together with AKT, is unknown.

To examine specifically the contributions of DSCR1 and the putative calcineurin-NF-AT-DSCR1 pathway to tumor progression and angiogenesis, we made use of mice with a targeted deletion of *both* DSCR1 isoforms (Ryeom et al., 2003). Inactivation of *DSCR1*, encoding both *DSCR1.Ex1* and *DSCR1.Ex4* isoforms, elicits a low-penetrance developmental defect associated with cerebral vascular degeneration. Importantly, however, the great majority of mice survive into adulthood but exhibit elevated and persistent activation of calcineurin. Such calcineurin hyperactivity triggers apoptosis of activated endothelial cells, with the effect of significantly suppressing subcutaneous and metastatic tumor growth by preventing the elaboration of stable tumor vasculature. Modest pharmacological suppression of calcineurin activity restores tumor growth in *DSCR1*$^{-/-}$ mice, confirming the idea that dysregulated calcineurin signaling in the vascular endothelium is directly responsible for suppressing tumor growth. Hence, the calcineurin-NF-AT-DSCR1 pathway constitutes a target for anticancer therapy.

RESULTS

Inactivation of DSCR1 Suppresses Tumor Growth

Since angiogenesis is necessary for macroscopic tumor expansion, we examined the impact of DSCR1 status on tumor growth in vivo. Murine renal carcinoma (RENCA) and colon carcinoma (MC26) tumor cells were inoculated into syngeneic *DSCR1* wild-type (WT) and *DSCR1*$^{-/-}$ mice and rates of growth measured over time. Growth of both RENCA and MC26 tumors was significantly retarded in *DSCR1*$^{-/-}$ mice relative to *DSCR1* WT controls (Figure 1A), with RENCA tumor growth more affected than that of MC26. One difference between these two tumor cell lines was that VEGF secretion was some 7-fold greater in RENCA versus MC26 tumors, as measured by ELISA (Figure 1B).

To establish whether differences in tumor growth were due to modulation of VEGF production by tumor cells in *DSCR1*$^{-/-}$ mice, we immunostained RENCA tumors from *DSCR1* WT and *DSCR1*$^{-/-}$ mice for VEGF but found no significant differences in similar sized tumors (Figure S1A available online). DSCR1 status in tumor vessels from *DSCR1* WT and *DSCR1*$^{-/-}$ mice was confirmed by costaining tumor tissue sections with anti-CD31 and anti-DSCR1 antibodies. DSCR1 colocalized with CD31 in tumors harvested from wild-type mice but was absent from tumors derived from *DSCR1*$^{-/-}$ animals (Figure 1C). Microvessel density was considerably increased in both RENCA and MC26 tumors isolated from wild-type mice versus tumors harvested from *DSCR1*$^{-/-}$ animals at the same time after tumor cell inoculation (Figure 1D; Figure S1C). Finally, to ensure that tumor growth was suppressed and not merely delayed in *DSCR1*$^{-/-}$ mice, we allowed MC26 colon carcinoma tumors in the *DSCR1*$^{-/-}$ mice to continue to grow for 2 weeks after their *DSCR1* WT equivalents had been euthanized because of large tumor burden (Figures S1B and S1C). At this time (day 31 after tumor cell inoculation) all tumors in *DSCR1*$^{-/-}$ mice appeared necrotic (Figure S1C) and exhibited similar tumor volumes as on day 15 (Figure S1B), consistent with suppression of tumor growth due to the inability to form and maintain a stable tumor vasculature. To confirm this, RENCA and MC26 tumors were harvested from WT and *DSCR1*$^{-/-}$ mice and coimmunostained with the endothelial-specific marker CD31 and for TUNEL reactivity to identify apoptotic endothelial cells. Tumors from *DSCR1*$^{-/-}$ mice generally had shorter, stunted vessels with most of the endothelial cells in longer vessels colocalizing with TUNEL-positive staining (Figure 1E; Figure S1D).

Blood vessel maturation is characterized by endothelial cells surrounded by smooth muscle cells and pericytes as indicated by alpha smooth muscle actin (αSMA) immunostaining (Ozawa et al., 2005). Tumors from *DSCR1*$^{-/-}$ mice demonstrated a significant reduction in SMA-positive and CD31-double-positive blood vessels (Figure 1F) as compared to tumors from wild-type mice. To characterize further the extent of tumor neovascularization in *DSCR1* WT versus *DSCR1*$^{-/-}$ mice, we used an in vivo tumor Miles permeability assay. Tumor-bearing mice were injected intravenously with Evans blue dye and, 30 min later, perfused with saline to remove dye from the vascular lumen. Tumors were then harvested and dye extracted and quantified spectrophotometrically. After normalization to tumor size and weight, we found significantly more dye present in tumors from *DSCR1* WT mice relative to their *DSCR1*$^{-/-}$ counterparts (Figure 1G), implicating the presence of a more extensive vascular network in tumors harvested from wild-type mice allowing the accumulation of more dye.

Calcineurin Signaling in Endothelial Cells Is Hyperactive in the Absence of DSCR1

To explore directly the role of DSCR1 in attenuating VEGF signaling, we isolated primary microvascular endothelial cells from both *DSCR1* WT and *DSCR1*$^{-/-}$ mice and compared the dynamics of VEGF-calcineurin signaling in vitro. Endothelial cell identity was confirmed by both morphology and immunofluorescence analysis using an anti-VEGFR2 antibody (Figures S2A and S2B). The absence of DSCR1 expression in *DSCR1*$^{-/-}$ endothelial cells was confirmed by immunofluorescence (Figure S2C) and western blotting using a DSCR1-specific monoclonal antibody (Ryeom et al., 2003). *DSCR1* WT endothelial cells treated with 10 ng/ml VEGF for 1 hr demonstrated expression of the inducible, 25 kDa DSCR1 isoform (*DSCR1.Ex4)*, while similarly treated *DSCR1*$^{-/-}$ endothelial cells expressed neither constitutive (38 kDa; *DSCR1.Ex1*) nor inducible DSCR1 isoforms (Figure 2A).

Since calcineurin signaling is mediated via nuclear import of the NF-AT transcription factor family, we next examined the kinetics

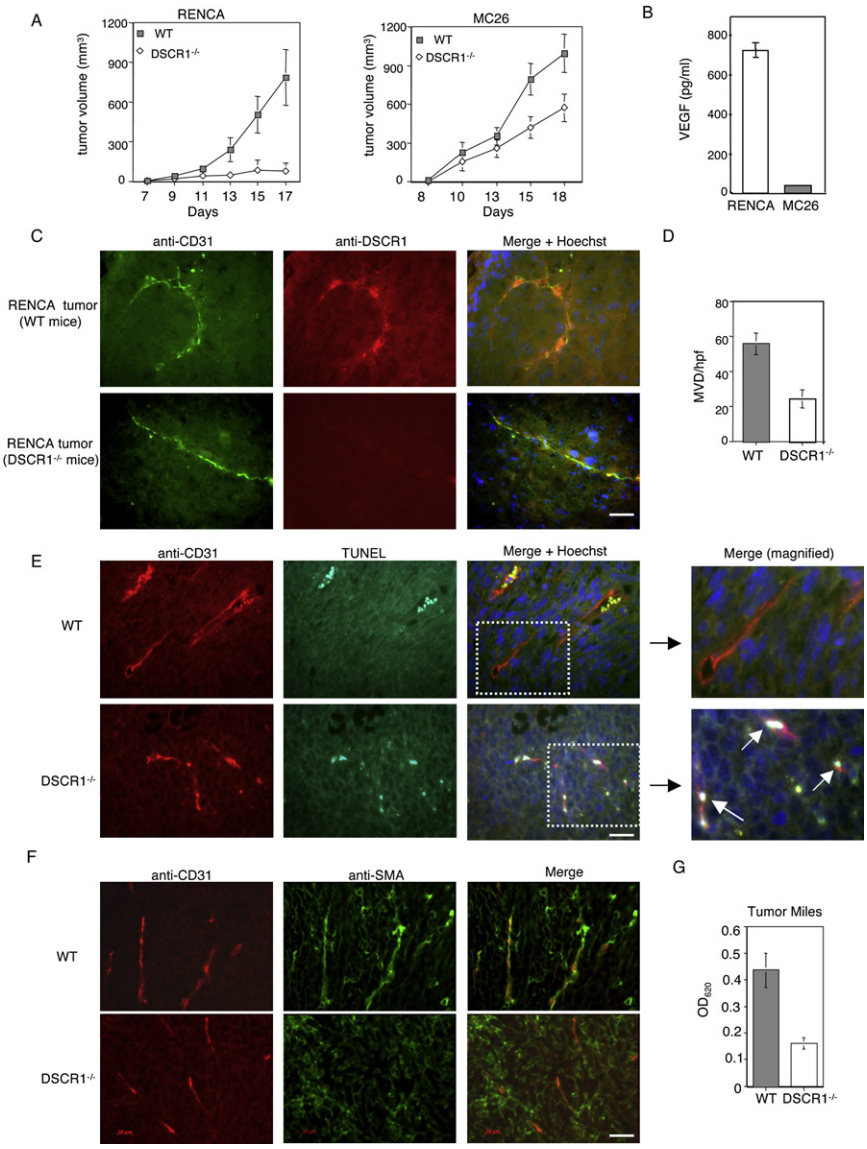

Figure 1. Tumor Angiogenesis Is Suppressed in *DSCR1*$^{-/-}$ Mice

(A) Subcutaneous tumor growth of two different syngeneic mouse tumor cells, renal cell carcinoma (RENCA) and colon carcinoma (MC26), was impaired in *DSCR1*$^{-/-}$ mice.

(B) VEGF production by RENCA and MC26 tumor cells as measured by ELISA.

(C) RENCA tumors harvested from WT and *DSCR1*$^{-/-}$ mice are coimmunostained with anti-CD31 and anti-DSCR1. Scale bar, 50 μM.

(D) Microvessel density (MVD) per high-powered field (hpf) of MC26 tumors harvested from *DSCR1*$^{-/-}$ animals was significantly reduced as compared to tumors from WT mice.

(E) RENCA tumors from *DSCR1* WT mice showed almost no TUNEL-positive cells, while RENCA tumors from *DSCR1*$^{-/-}$ mice show colocalization of the endothelial-specific marker CD31 and TUNEL reactivity (arrows) indicating apoptotic cells. Scale bar, 50 μM.

(F) Microvessel integrity was impaired in tumors harvested from *DSCR1*$^{-/-}$ animals as demonstrated by decreased colocalization of CD31 and alpha smooth muscle actin (αSMA) immunofluorescence. Scale bar, 50 μM.

(G) Tumors from *DSCR1* WT mice with more extensive vasculature have significantly higher levels of Evans blue dye compared to tumors from *DSCR1*$^{-/-}$ mice. All data are represented as mean ± SEM.

of endogenous NF-AT translocation in *DSCR1* WT and *DSCR1*$^{-/-}$ endothelial cells. NF-AT nuclear import has been reported after VEGF treatment of endothelial cells for 30 min in a calcineurin-dependent manner (Hernandez et al., 2001; Johnson et al., 2003). Within 5 min of VEGF exposure, 39.2% (±1.4) of *DSCR1*$^{-/-}$ endothelial cells exhibited NF-ATc1 nuclear localization as compared to only 7.9% (±4.0) of wild-type endothelial cells (Figure 2B). Indeed, even untreated *DSCR1*$^{-/-}$ endothelial cells showed some NF-ATc1 nuclear localization (Figure 2C), consistent with the notion that calcineurin is hyperactivated in *DSCR1*$^{-/-}$ cells even in the absence of a calcium agonist. Therefore, to ascertain that the precocious NF-ATc1 nuclear localization that we observed in *DSCR1*$^{-/-}$ endothelial cells was indeed dependent on calcineurin, we treated *DSCR1*$^{-/-}$ cells with the pharmacological calcineurin inhibitor cyclosporin A (CsA) (Liu et al., 1999). This dramatically reduced the proportion of *DSCR1*$^{-/-}$ cells exhibiting nuclear NF-ATc1 5 min after VEGF exposure to only 3.3% (±0.5) (Figures 2B and 2C).

To confirm the biological significance of the premature nuclear import of NF-ATc1 in *DSCR1*$^{-/-}$ endothelial cells, we examined expression of the proangiogenic NF-AT target gene *cyclooxygenase-2* (*Cox-2*) (Hernandez et al., 2001). Compared with *DSCR1* WT endothelial cells, Cox-2 expression was significantly upregulated in *DSCR1*$^{-/-}$ endothelial cells within only 15 min of VEGF exposure (Figure 2D). Thus, DSCR1 modulates expression of proangiogenic genes regulated by the VEGF-calcineurin-NF-AT pathway.

Finally, we assessed whether the absence of DSCR1 increased the sensitivity of endothelial cells to VEGF signaling. Indeed, exposure of *DSCR1* WT cells to low-dose VEGF (1–2.5 ng/ml) had negligible impact on ^{3}H-thymidine incorporation but potently promoted proliferation of their *DSCR1*$^{-/-}$ counterparts (Figure 2E). Thus, the absence of *DSCR1* significantly sensitizes cells to VEGF-induced signaling, most likely due to an inability to attenuate VEGF-calcineurin signaling.

Hyperactivation of the VEGF-Calcineurin-NF-AT Pathway in DSCR1-Deficient Endothelial Cells Suppresses Proliferation

While a simple model might suggest that hypersensitivity to VEGF might promote VEGF-induced endothelial cell proliferation, evidence suggests that the opposite may be true, in the main because constitutive activation of calcineurin is a potent inducer

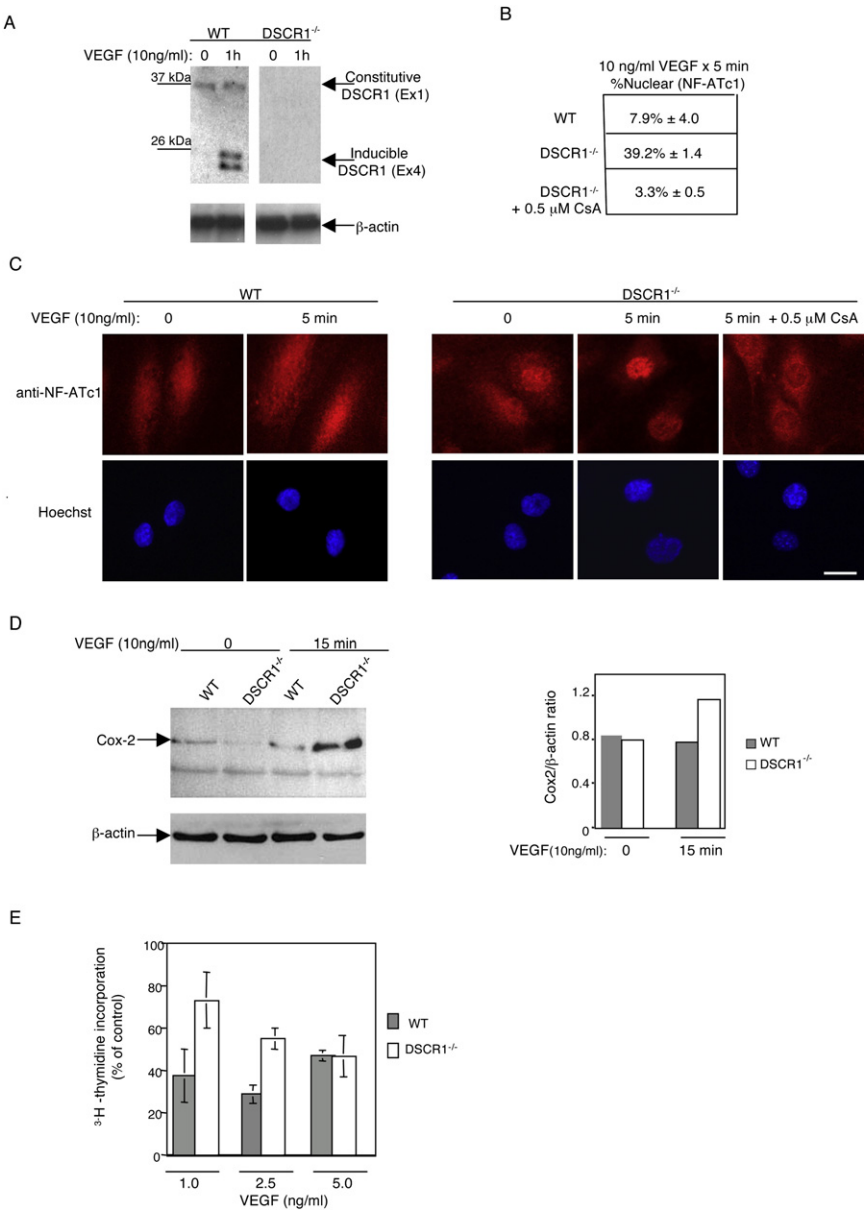

Figure 2. Hyperactivated Calcineurin Signaling in *DSCR1*$^{-/-}$ Endothelial Cells

(A) Western blot analysis of *DSCR1* WT and *DSCR1*$^{-/-}$ endothelial cell lysates probed with anti-DSCR1 monoclonal antibody, with or without VEGF (10 ng/ml) treatment for 1 hr. Blots were reprobed with β-actin as a loading control.

(B) Quantification of NF-ATc1 nuclear localization in *DSCR1* WT and *DSCR1*$^{-/-}$ endothelial cells after treatment with VEGF (10 ng/ml) with or without 0.5 μM cyclosporin A (CsA) for 5 min. Percent of cells with nuclear NF-ATc1 expression indicated as mean ± SEM.

(C) Subcellular localization of NF-ATc1 following VEGF treatment (10 ng/ml) of endothelial cells after 5 min with and without 0.5 μM CsA. Hoechst staining reveals nuclei. Scale bar, 20 μM.

(D) Representative western blot of Cox-2 expression in *DSCR1* WT and *DSCR1*$^{-/-}$ endothelial cells after VEGF treatment for 15 min. Blots were reprobed with β-actin as a loading control. Densitometric ratio of Cox2/β-actin signal in *DSCR1* WT and *DSCR1*$^{-/-}$ endothelial cell lysates (right).

(E) ^{3}H-thymidine uptake by *DSCR1* WT and *DSCR1*$^{-/-}$ endothelial cells after 3 days with basal media supplemented with low concentrations of VEGF. Data are represented as mean ± SEM.

of apoptosis (Wang et al., 1999). Consistent with this, exposure to mitogenic levels of VEGF (50–500 ng/ml) induced considerably greater expansion in numbers of *DSCR1* WT versus *DSCR1*$^{-/-}$ primary endothelial cells after 3 days (Figure 3A), indicating a deficit in VEGF-induced expansion of *DSCR1*$^{-/-}$ endothelial cells.

To ascertain whether this deficit in *DSCR1*$^{-/-}$ cell proliferation was dependent on calcineurin, we asked whether it could be reversed with the calcineurin inhibitor CsA. However, since normal calcineurin function is required for VEGF-induced endothelial cell proliferation, we first had to identify a concentration of CsA that dampens but did not completely eliminate calcineurin activity. Proliferation of wild-type endothelial cells was examined after 3 days exposure to 100 ng/ml VEGF treatment in the presence of CsA concentrations ranging from 25 nM to 500 nM (Figure S3). This indicated that CsA doses as low as 25 nM suppressed VEGF-induced cell proliferation. However, 10 nM CsA treatment effectively rescued the deficient VEGF-mediated growth of *DSCR1*$^{-/-}$ endothelial cells without

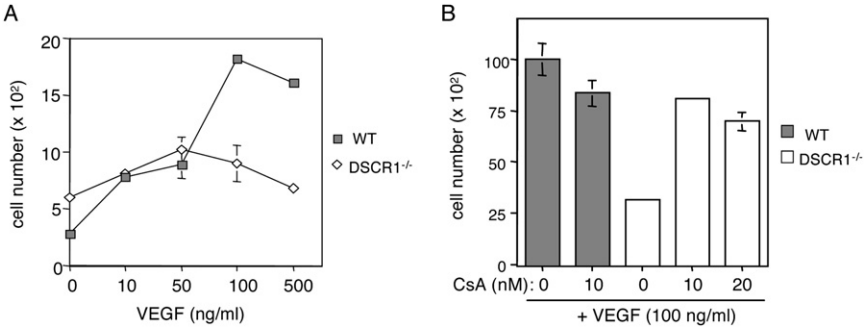

Figure 3. *DSCR1*$^{-/-}$ Endothelial Cells Demonstrate a Defect in VEGF-Mediated Proliferation that Is Rescued by Cyclosporin A Treatment

(A) Growth of *DSCR1* WT and *DSCR1*$^{-/-}$ endothelial cells after 3 days in vitro in basal media supplemented with the indicated concentrations of VEGF.

(B) Low-dose cyclosporin A (CsA) (10 nM) treatment rescued the proliferation defect seen in *DSCR1*$^{-/-}$ endothelial cells. All data are represented as mean ± SEM.

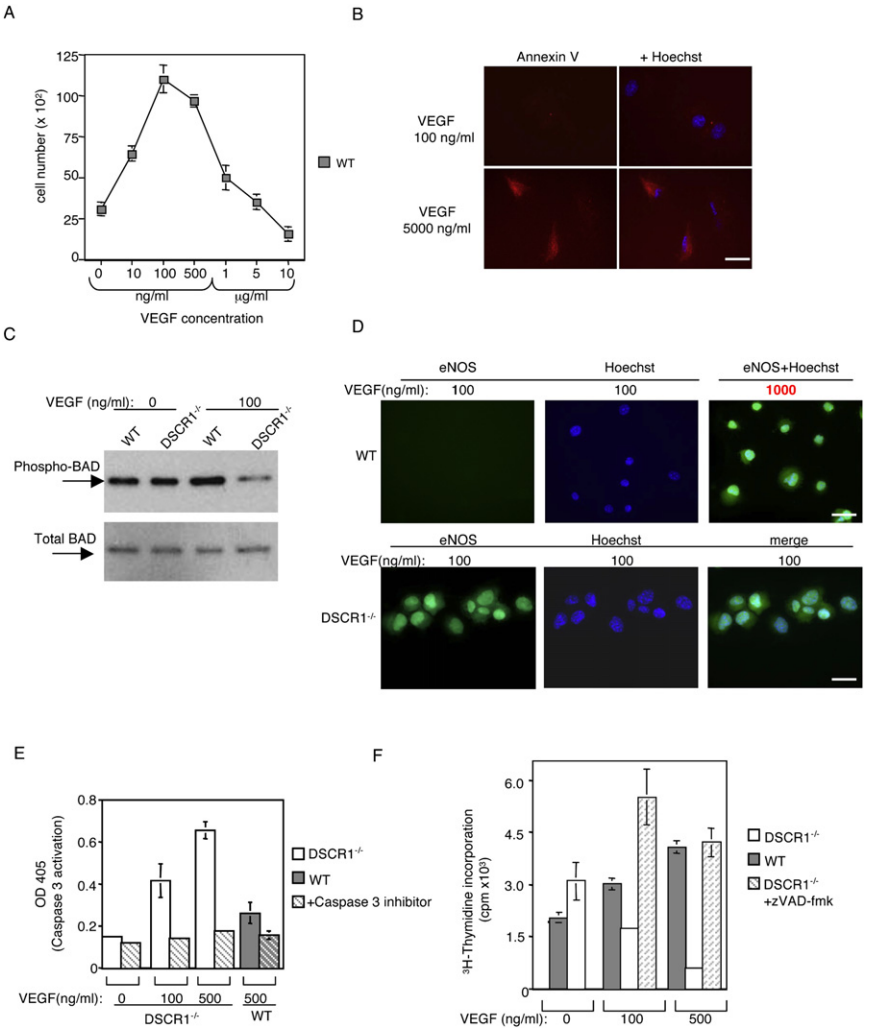

Figure 4. VEGF Induction of Apoptosis in Endothelial Cells

(A) Proliferation of endothelial cells (HMVEC) after 3 days in vitro in basal media supplemented with the indicated concentrations of VEGF. Data are represented as mean ± SEM.

(B) Annexin V and Hoechst immunofluorescence of HMVEC after treatment with the indicated concentrations of VEGF for 48–72 hr. Scale bar, 25 μM.

(C) Phospho-BAD levels are decreased in *DSCR1*$^{-/-}$ endothelial cells as compared to *DSCR1* WT endothelial cells after VEGF treatment for 48–72 hr.

(D) *DSCR1*$^{-/-}$ endothelial cells (bottom row) demonstrate upregulated inducible nitric oxide synthase (eNOS) expression in response to 100 ng/ml VEGF as compared to *DSCR1* WT endothelial cells (top row). *DSCR1* WT endothelial cells only express eNOS after treatment with 1000 ng/ml VEGF. Scale bar, 25 μM.

(E) Caspase-3 activity is significantly upregulated in *DSCR1*$^{-/-}$ endothelial cells after VEGF treatment and blocked by a caspase-3 inhibitor. Data are represented as mean ± SEM.

(F) VEGF-induced proliferation defect of *DSCR1*$^{-/-}$ endothelial cells is reversed by treatment with the caspase inhibitor, zVAD-fmk. Data are represented as mean ± SEM.

significantly affecting proliferation of wild-type endothelial cells (Figure 3B). Taken together, these data confirm that the proliferation defect observed in *DSCR1*$^{-/-}$ endothelial cells is indeed calcineurin dependent.

Hyperactivation of the VEGF-Calcineurin-NF-AT Pathway Triggers Apoptosis in DSCR1-Deficient Endothelial Cells

The failure of *DSCR1*$^{-/-}$ endothelial cell cultures to expand under the influence of VEGF could be due to decreased proliferation and/or increased apoptosis. To examine these possibilities, we initially measured cell viability by determining ATP content of *DSCR1*$^{-/-}$ cultures after 3 days exposure to VEGF. In the presence of increasing concentrations of VEGF, *DSCR1*$^{-/-}$ endothelial cells demonstrated decreased levels of ATP, further confirming a lack of endothelial cell expansion (Figure S4A).

Interestingly, the effects of DSCR1 inactivation could be recapitulated by exposing wild-type endothelial cells to extremely high levels of VEGF, which presumably overrides the DSCR1 feedback attenuation. At VEGF levels of 100 ng/ml VEGF and higher, we observed significant suppression of growth in WT endothelial cell cultures, similar to that observed in *DSCR1*$^{-/-}$ cells, albeit at 10-fold lower VEGF concentrations (Figure 4A). Annexin V immunostaining confirmed that this was due to apoptosis (Figure 4B). Thus, we postulated that non-physiologically high levels of VEGF phenocopy the effect of DSCR1 inactivation in *DSCR1* WT endothelial cells, so we next examined *DSCR1*$^{-/-}$ endothelial cell apoptosis after VEGF treatment.

In addition to its actions on NF-AT, calcineurin directly dephosphorylates the proapoptotic protein BAD, thus promoting its proapoptotic activity through neutralization of Bcl-x_L and, ultimately, caspase-3 activation and apoptosis (Wang et al., 1999) (Figure S4B). To determine whether BAD dephosphorylation could play a role in apoptosis of VEGF-treated *DSCR1*$^{-/-}$ cells, we directly examined phospho-BAD levels in WT and *DSCR1*$^{-/-}$ endothelial cells with and without VEGF exposure (100 ng/ml). Total cytoplasmic BAD was immunoprecipitated followed by western blot analysis with a phospho-BAD-specific antibody (Figure 4C). While there was no significant difference in phospho-BAD levels between untreated WT or *DSCR1*$^{-/-}$ endothelial cells, the proportion of total Bad phosphorylated was sharply decreased in *DSCR1*$^{-/-}$ (but not *DSCR1* WT) endothelial cells after VEGF treatment (Figure 4C; Figure S4C). These data are consistent with a direct role for hyperactive calcineurin signaling in promoting apoptosis through BAD activation.

Calcineurin is also known to regulate apoptosis in endothelial cells via the nitric oxide pathway. Calcineurin-mediated NF-AT dephosphorylation allows NF-AT to transactivate endothelial

nitric oxide synthase (eNOS) (Ritter et al., 2003) (Figure S4B). Under physiological conditions, eNOS and nitric oxide (NO) can stimulate endothelial proliferation and migration. However, at high concentrations, NO is proapoptotic in several tissue types, including endothelium (Dimmeler and Zeiher, 1999). To determine whether eNOS and NO production are upregulated in *DSCR1*$^{-/-}$ endothelial cells, we utilized the small molecule dye 4,5-diaminofluorescein diacetate (DAF-2DA), which is cleaved by eNOS emitting a fluorescence signal that is quantitatively dependent upon NO production in the cell (Rossig et al., 2002). After 100 ng/ml VEGF treatment for 24–36 hr, DAF-2DA fluorescence was significantly greater in *DSCR1*$^{-/-}$ versus *DSCR1* WT endothelial cells (Figure 4D). However, upregulation of DAF-2DA fluorescence was observed in *DSCR1* WT endothelial cells by exposing *DSCR1* WT endothelial cells to 10-fold higher levels of VEGF (1000 ng/ml), which again presumably overrides normal DSCR1 feedback attenuation (Figure 4D).

Both eNOS and BAD signaling converge on activation of caspase-3, a key effector of the execution phase of apoptosis (Porter and Janicke, 1999) (Figure S4B). We therefore assayed caspase-3 activity spectrophotometrically in VEGF-treated *DSCR1* WT and *DSCR1*$^{-/-}$ endothelial cells using a p-nitroaniline chromophore-based assay (Gurtu et al., 1997). Caspase-3 activity was confirmed by blocking with the caspase-3-specific inhibitor DEVD-fmk. Caspase-3 activity was significantly elevated in *DSCR1*$^{-/-}$ endothelial cells 36–48 hr after VEGF treatment (100 and 500 ng/ml) as compared to wild-type endothelial cells (Figure 4E). Furthermore, treatment of *DSCR1*$^{-/-}$ endothelial cell cultures with the broad pan-caspase inhibitor zVAD-fmk rescued the VEGF-induced growth defect in *DSCR1*$^{-/-}$ endothelial cells (Figure 4F).

Tumor Growth in *DSCR1*$^{-/-}$ Mice Is Restored upon Suppression of Calcineurin Signaling

Finally, to ascertain whether hyperactivate calcineurin signaling was causally responsible for suppressing tumor growth in *DSCR1*$^{-/-}$ mice, we asked whether systemic treatment of *DSCR1*$^{-/-}$ mice with the calcineurin inhibitor CsA could restore tumor growth and angiogenesis. Mice were inoculated subcutaneously with RENCA tumor cells and then treated daily by oral gavage with either low-dose (5 mg/kg) CsA (*DSCR1*$^{-/-}$ mice) or vehicle alone (WT and *DSCR1*$^{-/-}$ mice). Low-dose CsA was utilized to prevent any tumor-promoting effects observed with high-dose CsA (Hojo et al., 1999). Rapid tumor growth was restored in *DSCR1*$^{-/-}$ mice treated with CsA (Figures 5A–5C)—representative tumor weights and images are shown 28 days after tumor cell injection (Figures 5B and 5C). Furthermore, immunofluorescence analysis with anti-CD31 antibody and TUNEL reactivity confirmed that CsA treatment significantly suppressed apoptosis in endothelial cells of vessels from tumors grown in *DSCR1*$^{-/-}$ mice (Figures 5D and 5E).

To confirm that these findings were reproducible in other tumor models, we utilized a metastatic tumor model, by tail vein injection of murine MC26 colon carcinoma cells into syngeneic *DSCR1* WT and *DSCR1*$^{-/-}$ mice. Similar to our subcutaneous tumor model, the lungs of *DSCR1* WT mice demonstrated significant tumor burden as compared to *DSCR1*$^{-/-}$ mice as assessed by gross and histological analysis (Figures S5A–S5C). Low-dose CsA (5 mg/kg) treatment of *DSCR1*$^{-/-}$ mice restored

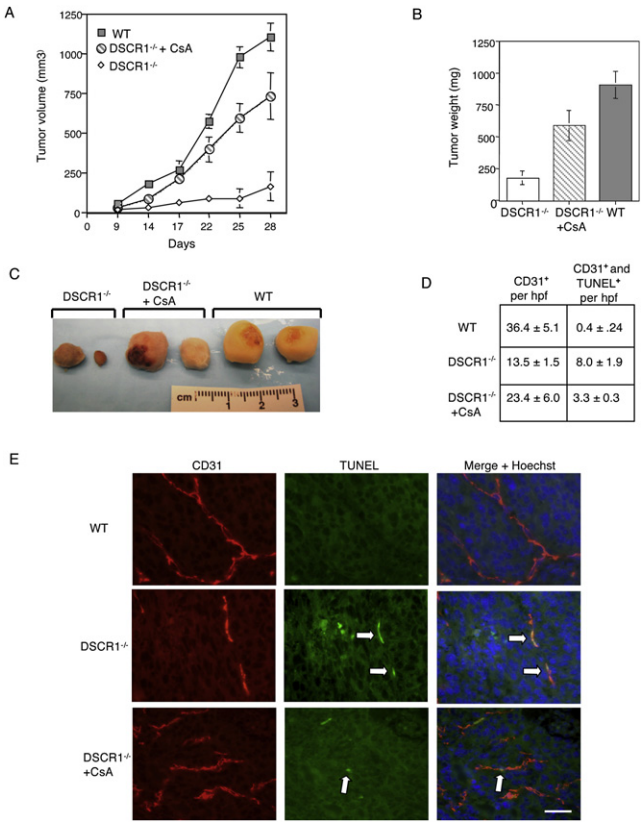

Figure 5. Low-Dose Cyclosporin A Treatment Can Compensate for Loss of DSCR1

(A) Subcutaneous tumor growth of the syngeneic mouse renal cell carcinoma (RENCA) is restored in *DSCR1*$^{-/-}$ mice when mice are treated with daily low-dose cyclosporin A (CsA) (5 mg/kg) by oral gavage. Data are represented as mean ± SEM.

(B) Average tumor weights 28 days after tumor cell inoculation of RENCA tumors harvested from *DSCR1*$^{-/-}$ mice treated with vehicle alone, *DSCR1*$^{-/-}$ mice treated with daily low-dose CsA, and *DSCR1* WT mice treated with vehicle alone. Data are represented as mean ± SEM.

(C) Representative images of tumors harvested from the indicated group.

(D) Quantification of CD31- and TUNEL-positive cells in RENCA tumors harvested from the indicated mice. Data are represented as mean ± SEM.

(E) RENCA tumors were immunostained for CD31 and TUNEL reactivity demonstrating increased CD31-positive cells and decreased CD31+/TUNEL double-positive cells in *DSCR1*$^{-/-}$ mice treated with daily low-dose CsA as compared to *DSCR1*$^{-/-}$ mice treated with vehicle alone. Scale bar, 50 μM.

growth of lung metastases comparable to that of *DSCR1* WT mice (Figures S5A, S5C, and S5D). Finally, anti-CD31 and TUNEL immunofluorescence demonstrated significantly fewer TUNEL-positive endothelial cells in lungs from *DSCR1*$^{-/-}$ mice treated with CsA versus *DSCR1*$^{-/-}$ mice treated with vehicle alone (Figures S5D and S5E).

DSCR1$^{-/-}$ Mice Demonstrate Decreased VEGF-Dependent Angiogenesis

Taken together, our data indicate that endogenous DSCR1 acts to attenuate VEGF signaling through calcineurin and NF-AT, thereby fostering VEGF-induced mitogenesis. In the absence

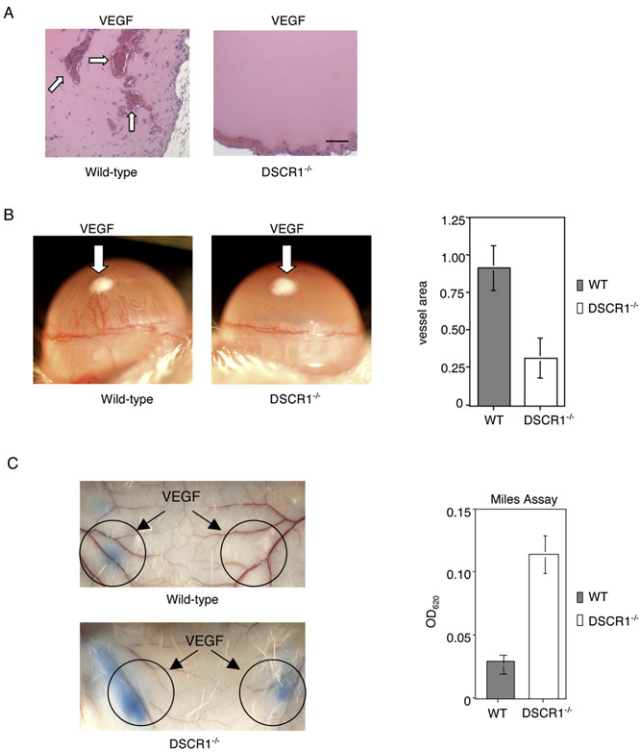

Figure 6. Decreased VEGF-Mediated Angiogenesis and Increased Vascular Permeability in *DSCR1*$^{-/-}$ Mice

(A) Increased vessel density in sections of Matrigel implants with VEGF after 7 days in *DSCR1* WT as compared to *DSCR1*$^{-/-}$ mice. Arrows indicate major vessels. Scale bar, 50 μM.

(B) Comparison of corneal angiogenesis following VEGF injection in *DSCR1* WT and *DSCR1*$^{-/-}$ mice. Arrow indicates VEGF pellet. The histogram (right) indicates quantification of vessel length and numbers. Data are represented as mean ± SD.

(C) Miles permeability assay demonstrates increased VEGF-induced vascular permeability in *DSCR1*$^{-/-}$ mice as compared to WT mice. The histogram (right) quantifies Trypan blue levels in the tissue. Data are represented as mean ± SD.

of DSCR1, VEGF signaling elicits precocious and persistent calcineurin activation, which triggers endothelial cell death, potentially through BAD activation and induction of eNOS (Figure 4C).

To explore the biological consequences of *DSCR1* inactivation on angiogenesis in vivo, we assayed its effects on VEGF-induced vessel growth in Matrigel implants and in the corneal eye assay (Figures 6A and 6B). *DSCR1*$^{-/-}$ mice exhibited a significant decrease in the numbers of vessels invading Matrigel pellets and in response to VEGF pellets in the corneal eye assay, compared with *DSCR1* WT mice (Figures 6A and 6B). To examine the influence of DSCR1 status on vascular permeability in response to VEGF, we used the Miles permeability assay. VEGF (50 μl; 1 ng/μl) was injected into the skin, and Evans blue levels in the vessels and surrounding stroma were quantified spectrophotometrically. *DSCR1*$^{-/-}$ mice showed significantly increased levels of Evans blue dye in response to VEGF when compared with *DSCR1* WT mice (Figure 6C), consistent with defects in endothelial cell proliferation or viability (Hashizume et al., 2000).

Loss of DSCR1 Causes Cerebral Hemorrhage in Developing Embryos

Since angiogenesis is critical in embryonic development, we examined the effect of *DSCR1* loss during development. Mendelian ratios of pups derived from numerous *DSCR1*$^{+/-}$ matings were skewed, with fewer than the expected 25% of *DSCR1*$^{-/-}$ offspring and suggestive of a variable penetrance, lethal, developmental abnormality. Analysis at embryonic days 10 and 12 (E10 and E12) of >20 litters derived from *DSCR1* heterozygous and homozygous matings (n = 161 mice) revealed obvious cerebral hemorrhage in ~15% of *DSCR1*$^{-/-}$ embryos (Figure 7A), leading to death and resorption before birth (data not shown). Hematoxylin and eosin images of vessels in the brain of *DSCR1*$^{-/-}$ embryos at E10 and E12 show abrupt appearance of leaky vessels by E12, evident by extravasation of nucleated red blood cells into the surrounding tissue (Figure 7B). Furthermore, E12 *DSCR1*$^{-/-}$ embryos exhibit blood-filled ventricles that are absent in *DSCR1* WT embryos at E12 (Figure 7C). Immunofluorescence analysis using anti-DSCR1 mAb confirmed expression of DSCR1 in endothelial cells lining vessels of WT E12 embryos that is absent from *DSCR1*$^{-/-}$ siblings (Figure 7D).

Previous studies have demonstrated that initiation of heart valve morphogenesis at E9 requires calcineurin-NF-AT signaling to repress VEGF expression in the myocardium and allow transformation of endocardial cells into mesenchymal cells (Chang et al., 2004). To determine how loss of DSCR1 might affect VEGF levels in the embryo, we measured VEGF production in E11 *DSCR1* WT and *DSCR1*$^{-/-}$ embryos by ELISA and found VEGF to be significantly upregulated in *DSCR1*$^{-/-}$ embryos (Figure 7E). This increase in VEGF expression in *DSCR1*$^{-/-}$ hearts was confirmed by anti-VEGF immunofluorescence on sections of E11 heart from *DSCR1*$^{+/+}$ and *DSCR1*$^{-/-}$ mice (Figure 7F).

DISCUSSION

The pivotal importance played by angiogenesis in providing necessary oxygen and nutrients for the expansion and spread of tumors is widely accepted (Folkman et al., 2006). Endothelial cells comprise the principal component of blood vessels, and tumor angiogenesis is driven by their proliferation and migration in response to proangiogenic cytokines produced by both tumor and stromal cells (Folkman et al., 2006). Interference with tumor angiogenesis has now emerged as an important and mechanistically distinct therapeutic strategy for treating cancer, thus focusing great interest on how angiogenic signals are generated by tumors, are sensed by endothelial cells, and exert their effects. Our studies have identified a role for VEGF signaling through the calcineurin-NF-AT pathway in the regulation of tumor angiogenesis and growth. In particular, we have uncovered the critical importance of DSCR1, the Down syndrome candidate region-1 protein, as an endogenous attenuator of the calcineurin-NF-AT pathway in the endothelium. Remarkably, inactivation of DSCR1 leads to elevated and persistent activation of calcineurin-NF-AT signaling, which triggers endothelial cell death rather than mitogenesis and acts as a potent inhibitor of tumor growth. Our data identify DSCR1 as a potential target for antiangiogenic cancer therapy.

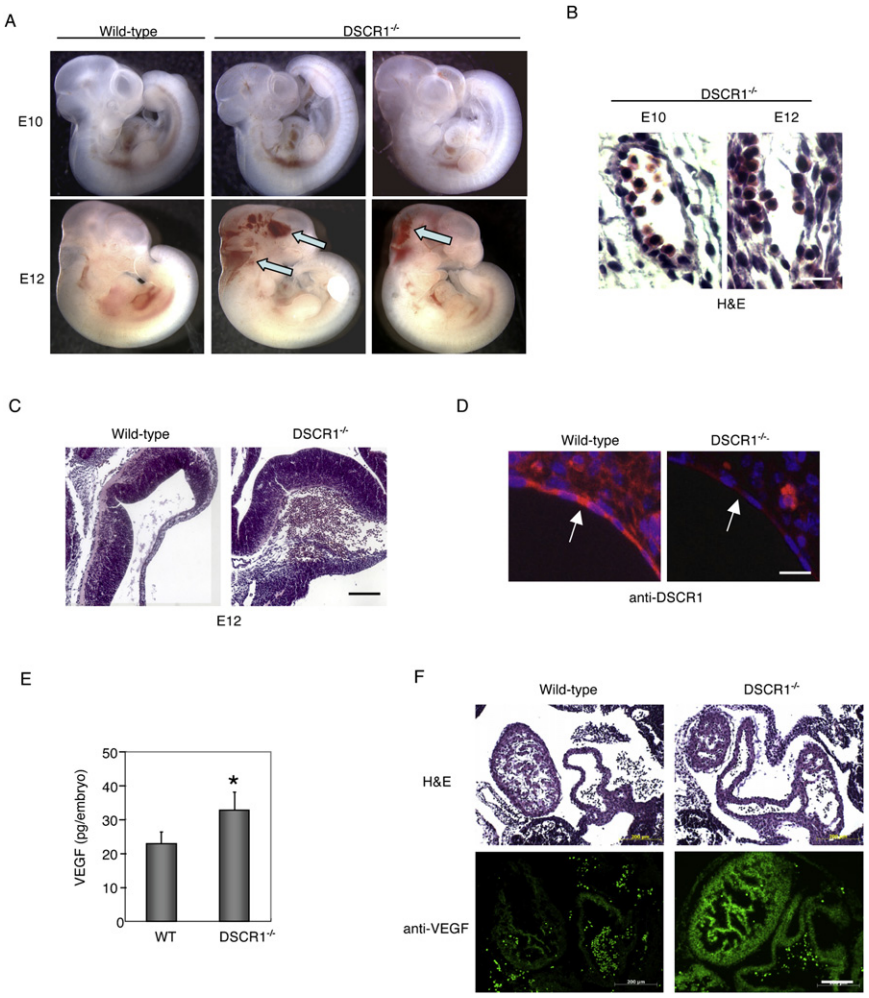

Figure 7. Loss of DSCR1 Leads to Cerebral Hemorrhage in Developing Embryos

(A) Approximately 15% of *DSCR1*$^{-/-}$ embryos demonstrate cerebral hemorrhages (arrows) at embryonic day 12 (E12) as compared to embryonic day 10 (E10).

(B) H&E images of vessels in the brain of *DSCR1*$^{-/-}$ embryos at E10 and E12 demonstrate leaky vessels at E12 as indicated by nucleated red blood cells in the surrounding tissue. Scale bar, 40 μM.

(C) H&E image of blood-filled ventricles in *DSCR1*$^{-/-}$ embryos as compared to wild-type embryos at E12. Scale bar, 200 μM.

(D) Anti-DSCR1 mAb immunofluorescence analysis of sections from *DSCR1* WT and *DSCR1*$^{-/-}$ mice demonstrate DSCR1 expression in endothelial cells lining large vessels in wild-type mice. Scale bar, 40 μM.

(E) VEGF levels are significantly increased in E11 *DSCR1*$^{-/-}$ embryos as compared to *DSCR1* WT embryos measured by ELISA (*$p < 0.05$). Data are represented as mean ± SD.

(F) Anti-VEGF immunofluorescence of the developing heart at E11 in *DSCR1* WT and *DSCR1*$^{-/-}$ mice. Images were captured using the same exposure time, indicating increased VEGF expression in *DSCR1*$^{-/-}$ hearts. Scale bar, 200 μM.

Previous studies have shown that ectopic overexpression of DSCR1 binds to, and potently suppresses, calcineurin activation—in turn, blocking nuclear relocalization and activity of the NF-AT transcription factor (Iizuka et al., 2004; Hesser et al., 2004; Minami et al., 2004; Yao and Duh, 2004). Since NF-AT directly transactivates the inducible isoform of *DSCR1*, *DSCR1.Ex4* (Iizuka et al., 2004; Hesser et al., 2004; Minami et al., 2004; Yao and Duh, 2004), the potential exists for a physiological negative feedback loop by which induction of *DSCR1* attenuates calcineurin-NF-AT signaling. To investigate this possibility in normal endothelial cells, we assayed calcineurin activation via subcellular localization of NF-ATc1 after VEGF treatment of endothelial cells. VEGF exposure induced rapid (within 30 min) localization of NF-AT to the endothelial cell nucleus, as expected. However, despite sustained exposure of cells to VEGF and, presumably, persistent elevation of intracellular calcium, NF-AT relocalized back to the cytosol at later times (Figure S6A). Such relocalization indicates attenuation of the calcineurin signal and coincides temporally with the delayed (~1 hr), NF-AT-dependent induction of *DSCR1.Ex4* expression (Figures S6B and S6C). These data suggested a model whereby *DSCR1.Ex4* induction attenuates VEGF signaling by downregulating calcineurin activity. To confirm this, we examined the level and persistence of calcineurin-NF-AT signaling in endothelial cells deficient in DSCR1. As predicted, *DSCR1*$^{-/-}$ cells exhibited increased rapidity of response and sensitivity to VEGF-induced NF-AT nuclear localization and induction of NF-AT target genes, which was abrogated by cotreatment of cells with the calcineurin inhibitor CsA.

Perhaps surprisingly, germline deletion of *DSCR1* elicited rather mild phenotypic effects—the majority of *DSCR1*$^{-/-}$ mice were normal, but ~15% exhibited a lethal cerebral hemorrhage phenotype. We speculate that VEGF levels during embryonic development of *DSCR1*$^{-/-}$ mice hover close to a threshold level necessary to trigger constitutive calcineurin activation. Consistent with this, VEGF levels in *DSCR1*$^{-/-}$ embryos are significantly higher than those of littermate *DSCR1* WT embryos. While loss of DSCR1 in the developing heart might be expected to trigger hyperactive calcineurin signaling and constitutive transrepression of VEGF via NF-AT (Chang et al., 2004), other studies have shown that DSCR1 has dual roles in the heart and can either potentiate or inhibit calcineurin signaling (Vega et al., 2002).

DSCR1-dependent physiological attenuation of VEGF-induced calcineurin-NF-AT activation may well serve some role in forestalling precocious endothelial cell activation during normal physiological spikes of circulating or paracrine VEGF. Surprisingly, however, hyperactivation of the calcineurin-NF-AT pathway did not lead to the obvious augmentation of growth responses of endothelial cells to VEGF: rather, *DSCR1*$^{-/-}$ endothelial cells exhibited a substantial decrease in cell expansion when exposed to VEGF due to the onset of endothelial apoptosis. This suggested that hyperactivation of calcineurin-NF-AT in *DSCR1*$^{-/-}$ cells reroutes downstream calcineurin/NF-AT output to engage cell death

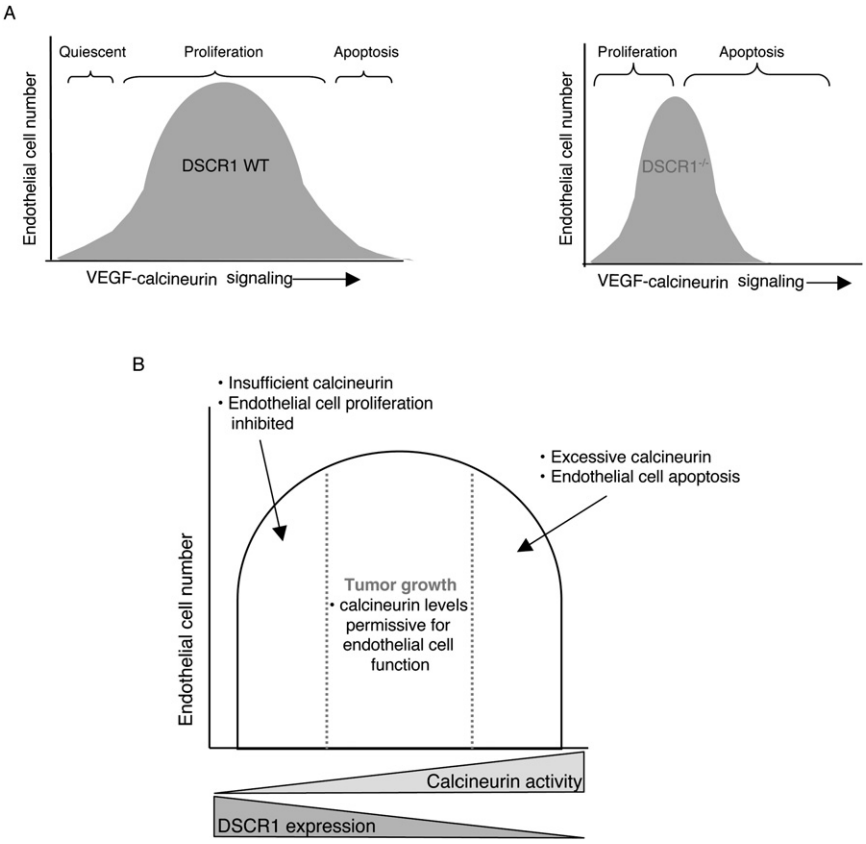

Figure 8. Model of VEGF-Calcineurin-DSCR1 Regulation of Endothelial Cell Function

(A) Model depicting endothelial cell behavior upon increasing VEGF-calcineurin signaling in the presence (left) and absence (right) of DSCR1.

(B) Model of tumor growth relative to DSCR1 levels and calcineurin activity in endothelial cells. As DSCR1 expression decreases, calcineurin activity increases. Tumor growth occurs with moderate levels of calcineurin activity in endothelial cells. Too little calcineurin activity blocks endothelial cell proliferation, and too much calcineurin activity triggers endothelial cell apoptosis.

machinery (Figure 8A). Further analysis identified two candidate pathways for this pathological cell death response—calcineurin-dependent dephosphorylation and activation of the BH3 pro-death protein BAD, and induction of the NF-AT target gene eNOS. The extent to which either of these two proapoptotic effectors contributes to the calcineurin hyperactivation apoptotic phenotype in endothelial cells requires further studies.

Since hyperactivation of the calcineurin-NF-AT pathway in *DSCR1*$^{-/-}$ mice drives endothelial apoptosis, we suspected that it might also limit the capacity of tumors to maintain a blood supply. We confirmed this by demonstrating a substantial inhibition in initiation and progression of transplanted tumors in *DSCR1*-deficient hosts. This suppression of tumor growth corresponded with deficits in vascular expansion and elaboration, as well as endothelial cell apoptosis, and was abrogated by systemic treatment of mice with the calcineurin inhibitor CsA. Our data do not exclude the possible roles of other mechanisms contributing to tumor suppression in *DSCR1*$^{-/-}$ mice. For example, a direct role for NF-AT transcription factors has been proposed in promoting invasion of breast cancers through inactivation of AKT signaling (Jauliac et al., 2002). However, examination of AKT activation in *DSCR1* WT and *DSCR1*$^{-/-}$ endothelial cells revealed no significant differences in phospho-AKT expression after VEGF treatment (data not shown), suggesting that DSCR plays no direct role in regulating activation of AKT in endothelial cells. The calcineurin-NF-AT-DSCR1 signaling pathway is also known to play a critical role in immune cell activation (Ryeom et al., 2003), which is thought to play an important role in tumor growth. However, crossing our *DSCR1*$^{-/-}$ mice into the immunocompromised SCID background (Bosma et al., 1988) had no effect on the inhibition of tumorigenesis afforded by DSCR1 deficiency (Figures S7A and S7B), excluding a significant role for T and B cells.

The idea that hyperactivation of VEGF signaling pathways may actually suppress endothelial cell growth is consistent with observations that the response of normal endothelial cells to VEGF is biphasic, with very high levels of VEGF triggering suppression of migration (Watanabe et al., 2004) and initiation of apoptosis (Figure 4B). More generally, the notion that an intermediate strength of VEGF signaling is required for efficacious angiogenesis is becoming an established and unifying theme. Conventional wisdom has dictated that more is generally better in chemotherapeutic treatment targeting cancer cells. However, recent studies utilizing antiangiogenic agents directed specifically at endothelial cells confirm a biphasic effect of these drugs (Folkman et al., 2006). If, as we predict, tumor angiogenesis requires an optimal and intermediate level of angiogenic signaling, even slight perturbations of VEGF signaling in the endothelium may prove to be an effective strategy for disrupting tumor growth (Figure 8B). The delicate nature of the equilibrium between DSCR1 and calcineurin-NF-AT suggests that the calcineurin-NF-AT-DSCR1 pathway may be an unusually sensitive target for antiangiogenic and anticancer therapies.

EXPERIMENTAL PROCEDURES

Generation of DSCR1 Null Mice

DSCR1$^{-/-}$ mice were generated as previously described (Ryeom et al., 2003), backcrossed ten generations, and maintained on C57Bl/6 and Balb/C backgrounds. All procedures were performed according to protocols approved by Children's Hospital Institutional Animal Care and Use Committee.

Endothelial Cell Isolation

Three- to four-week-old *DSCR1*$^{-/-}$ or WT mice were euthanized, and lungs were removed, minced, and digested in 625 U/ml collagenase II (GIBCO) in HBSS for 30 min at 37°C. Cells were strained through a 100 μm strainer, and collagenase activity was quenched with equal volume fetal calf serum. Cells were resuspended in 5 ml sterile HBSS, loaded on an equal volume of histopaque (Sigma) followed by centrifugation at 2000 rpm for 20 min. The

cloudy interface containing endothelial cells was removed and washed with sterile HBSS + 0.5% BSA. Cells were then resuspended in 400 μl HBSS + 0.5% BSA and 2 μl CD31-FITC mAb (PharMingen) and rotated for 30 min at 4°C. Endothelial cells were washed and resuspended in 90 μl of sterile MACS buffer (PBS + 0.5% BSA/2 mM EDTA). Ten microliters of anti-FITC mAb conjugated to magnetic beads (Miltenyi Corp.) was added to the cells and incubated for 15 min at 4°C. Next, 400 μl MACS buffer was added to each cell preparation, and the entire volume was applied to Miltenyi charcoal columns attached to a magnet so that CD31-bound cells adhered to the columns. Columns were washed three times and removed from the magnet, and cells were released into sterile tubes. CD31-bound cells were centrifuged at 1000 rpm for 5 min and resuspended in endothelial cell media (DMEM, 15 mM HEPES, heparin, ECGS [Biomedical Technologies], 20% FBS, 5mM glutamine-pen-strep) and plated into a gelatin-coated T-75 flask. Endothelial cells were reselected using FITC-lectin followed by incubation with anti-FITC-conjugated magnetic beads. The same protocol for reselection was followed as previously described for primary selection. Endothelial cell purity was determined by anti-VEGFR2 immunofluorescence, and cells were used for experiments between passages 2 and 6.

Proliferation

DSCR1$^{-/-}$ and WT endothelial cells or human microvascular endothelial cells (HMVEC; Cambrex) were plated at 12,500 cells per well in a 24-well tissue culture dish coated with 0.2% gelatin. Cells were incubated overnight in EBM (Cambrex) with 0.5% FBS followed by incubation in EBM with 0.5% FBS (supplemented with the indicated concentrations of recombinant VEGF [$VEGF_{165}$, NIH] or the indicated concentrations of CsA [Sigma]). Each condition was plated in triplicate, and cells were counted at the indicated times on a Coulter counter. Data are presented as the mean ± SEM. For ^{3}H-thymidine uptake, endothelial cells were plated 1 × 10^{4} cells/ml with 0.2% FBS for 14–18 hr followed by addition of the indicated concentration of recombinant VEGF or CsA for 24–48 hr. Cells were pulsed for 16–24 hr with 1 μCi/ml ^{3}H-thymidine, fixed in 10% (w/v) trichloroacetic acid, and solubilized in scintillation fluid and counted in a scintillation counter. Z-VAD-fmk (Alexis Biochemicals) was solubilized in DMSO and added at a final concentration of 20 μM.

Western Blot

Equal numbers of *DSCR1*$^{-/-}$ and WT endothelial cells were plated in 48-well dishes and treated with 10 μg/ml VEGF for the indicated times and lysed in sample buffer. Lysates were separated by SDS-PAGE, transferred to nitrocellulose membranes, and probed for DSCR1 expression (14B4 monoclonal antibody at 1:200) (Ryeom et al., 2003) and β-actin (1:10,000; Abcam). Blots were incubated with goat anti-mouse HRP-conjugated secondary (1:1000; Zymed) for 1 hr followed by ECL (Amersham) for signal detection.

For phospho-BAD and total BAD expression, 7500 *DSCR1*$^{-/-}$ and *DSCR1* WT endothelial cells were plated in 24-well tissue culture dishes and incubated in 0.1% FBS overnight followed by incubation with the indicated concentrations of recombinant $VEGF_{165}$ for 48 hr. Cells were lysed in 1% NP-40 with protease inhibitors, precleared with 50% slurry of washed sepharose beads in PBS, then incubated overnight at 4°C with 1 μg anti-BAD mAb (New England Biolabs) followed by a 2 hr incubation with 50% slurry of protein G-sepharose beads (Amersham). Beads were washed three times with 1% NP40 lysis buffer, resuspended in sample buffer, separated by SDS-PAGE, and probed with anti-Phospho-BAD antibody (New England Biolabs).

ATP Viability and Caspase-3 Assay

DSCR1$^{-/-}$ and WT endothelial cells (1 × 10^{6}) were plated in 96-well plates and stimulated with EBM plus 1% FBS and the indicated concentrations of VEGF. Cell viability was measured after 3 days with a luminescence ATP assay (Cell Titer-Glo, Promega) measuring release of ATP from live cells. Caspase-3 activity was measured after 36–48 hr following addition of cell lysis buffer as per the manufacturer's instructions (BD ApoAlert Caspase Colorimetric Assay Kit, Clontech). Caspase-3 activity was measured with the substrate DEVD-pNA and inhibited with DEVD-fmk. Absorbance was measured at 405 nm. Data are presented as the mean ± SEM.

Immunohistochemistry

Mice were euthanized and tumors were harvested and fixed in neutral-buffered formalin for paraffin sections. Formalin-fixed, paraffin-embedded tumor sections were deparaffinized by successive incubations in xylene, 95% ethanol, 90% ethanol, 70% ethanol followed by PBS. Epitopes were unmasked with 20 μg/ml proteinase K in PBS at room temperature (RT) for 30 min and rinsed twice in PBS with 0.3% Triton X-100 (PBS-T). Sections were immunostained with rat anti-CD31 mAb (1:50; PharMingen) or goat anti-mouse-αSMA mAb (1:500; Neomarkers) overnight at RT followed by incubation for 2 hr with goat anti-rat Alexa 594-conjugated secondary antibody (1:500; Molecular Probes) or goat anti-mouse Alexa 488 (1:500; Molecular Probes), respectively, for 2 hr at RT.

Sections were TUNEL stained using the Dead-End labeling kit (Promega) following the manufacturer's instructions. In brief, sections were incubated for 15 min in equilibration buffer followed by incubation with fluoresceinated rdNTPs and terminal deoxy transferase for 60 min at 37°C. Reactions were stopped by incubation in 2xSSC for 15 min followed by serial washes in PBS-T. Cell nuclei were stained with Hoechst dye (1 μg/ml; Sigma). Images were obtained on a Zeiss microscope and analyzed using AxioVision 4.0 software (Carl Zeiss Vision).

Immunofluorescence

Endothelial cells (10 × 10^{5}/ml) were plated onto gelatin-coated glass coverslips overnight. Cells were fixed with paraformaldehyde for 7 min at RT followed by blocking in 3% milk in Tris-buffered saline with Tween (TBS-T) for 45 min. Anti-VEGF-R2 mAb (1:500; Cell Signaling) or DSCR1 mAb (1:500) (Ryeom et al., 2003) or anti-Annexin V mAb (1:100; Santa Cruz) or isotype-matched control antibodies were added for 1 hr at RT. Endothelial cells stained with Annexin mAb were not permeabilized to detect cell surface expression of annexin V. Cells were washed with PBS-T before the addition of rabbit anti-mouse-Alexa 594 (1:500; Molecular Probes) for 30 min at RT protected from light. Nuclei were stained with 1% Hoechst dye for 1 min. Cells were extensively washed with PBS-T, mounted, and viewed on a fluorescence microscope. For uptake of 4,5-diaminofluorescein diacetate (DAF-2DA; Alexis Biochemicals), a fluorescent indicator of NO, endothelial cells were treated with the indicated conditions, washed free of serum, and incubated with DAF-2DA diluted in PBS (1:500) for 30–60 min, washed extensively, and viewed on a fluorescence microscope.

Matrigel Plug Assay

Matrigel plug assays were performed as described (Montrucchio et al., 2000). Briefly, Matrigel with VEGF (BD Bioscience) in liquid form at 4°C was injected (0.5 ml per mouse) intraperitoneally into wild-type and DSCR1 null mice along the midline. Mice were euthanized after 7 and 14 days, and gels were recovered and processed for histology.

Corneal Micropocket Assay

Corneal angiogenesis assays were performed as described (Kenyon et al., 1997). Eight- to ten-week-old DSCR1 null and wild-type mice were anesthetized, and topical anesthetic was applied to both eyes before incision with a 30° angle microknife. A pocket is made perpendicular to the incision with a von Graefe cataract knife. A 0.4 mm × 0.4 mm × 0.2 mm sucrose aluminum sulfate pellet coated with hydron polymer type NCC containing 160 ng VEGF was inserted into the pocket and implanted 0.7–1.0 mm from the limbus. Five days postsurgery, animals' eyes are examined with a slit lamp microscope and any vessel growth is measured.

Skin Miles Vascular Permeability Assay

Six- to eight-week-old mice were anesthetized and injected intravenously with 100 μl of a 1% Evans blue dye in normal saline solution. After 10 min, 1 ng/μl of recombinant VEGF165 (NIH) in 50 μl normal saline was injected intradermally into the shaved back of the mice. After 20 min mice were sacrificed, skin was removed, and equivalent-sized skin biopsies were placed in 500 μl formamide for 5 days at RT for complete extraction of blue dye. Concentration of dye was quantified by absorbance readings of 620 nm.

Tumor Miles Permeability Assay

Tumor-bearing mice were anesthetized and injected intravenously with 100 μl of a 1% Evans blue dye in normal saline solution. After 30 min, an 18 gauge cannula was inserted into the left ventricle, and an exit incision was made in the right atrium. Mice were perfused systemically with PBS for 30 min at a pressure of 120 mm Hg. Tumors was then removed and placed into 2 ml formamide

for 5 days to extract blue dye. The dye extrusion was quantified by absorbance at 620 nm with optical densitometry values normalized to tumor volume.

Tumor Models

Murine MC26, murine RENCA, or B16F10 melanoma cells (1×10^6) were injected subcutaneously into the flanks of 6- to 8-week-old DSCR1 null or wild-type mice. Tumors were measured with calipers, and volume was calculated by the formula TV = (length × width^2) × 0.52 (O'Reilly et al., 1997). For metastatic tumor models, 1×10^6 MC26 tumor cells were injected intravenously into 6- to 8-week-old *DSCR1*$^{-/-}$ or littermate WT mice. Mice were euthanized at the indicated days after tumor cell injection, and lungs were isolated, weighed, and fixed in neutral-buffered formalin for histology. Data are presented as the mean ± SEM.

CsA Treatment

Murine MC26 cells (1×10^6) were injected intravenously into 6- to 8-week-old *DSCR1*$^{-/-}$ or littermate WT mice. CsA (5 mg/kg in olive oil) was administered every other day by oral gavage starting on the day of tumor cell injection. On the indicated days after tumor inoculation, mice were euthanized, and pulmonary metastases and tumor burden were assessed grossly and histologically.

SUPPLEMENTAL DATA

The Supplemental Data include seven supplemental figures and can be found with this article online at http://www.cancercell.org/cgi/content/full/13/5/420/DC1/.

ACKNOWLEDGMENTS

This work is dedicated to the memory of Judah Folkman, an extraordinary scientist, physician, and mentor. We are indebted to G. Evan, K. Cichowski, and J. Folkman for advice and critical discussions. This work was supported by grants from the Richard and Susan Smith Family Foundation, Chestnut Hill, MA (S.R.); the Garrett B. Smith Foundation (S.R.); Massachusetts General Hospital Surgical Research Council Junior Faculty Award (S.S.Y.); and an ASCO Young Investigator Grant (S.S.Y.).

Received: January 15, 2007
Revised: December 31, 2007
Accepted: February 26, 2008
Published: May 5, 2008

REFERENCES

Abe, M., and Sato, Y. (2001). cDNA microarray analysis of the gene expression profile of VEGF-activated human umbilical vein endothelial cells. Angiogenesis *4*, 289–298.

Bosma, M., Schuler, W., and Bosma, G. (1988). The scid mouse mutant. Curr. Top. Microbiol. Immunol. *137*, 197–202.

Chang, C.P., Neilson, J.R., Bayle, J.H., Gestwicki, J.E., Kuo, A., Stankujnas, K., Graef, I.A., and Crabtree, G.R. (2004). A field of myocardial-endocardial NFAT signaling underlies heart valve morphogenesis. Cell *118*, 649–663.

Crabtree, G.R., and Olson, E.N. (2002). NFAT signaling: Choreographing the social lives of cells. Cell Suppl. *109*, S67–S79.

Dimmeler, S., and Zeiher, A.M. (1999). Nitric oxide—An endothelial cell survival factor. Cell Death Differ. *6*, 964–968.

Ferrara, N. (2004). Vascular endothelial growth factor: Basic science and clinical progress. Endocr. Rev. *25*, 581–611.

Ferrara, N., Gerber, H.P., and LeCouter, J. (2003). The biology of VEGF and its receptors. Nat. Med. *9*, 669–676.

Folkman, J., and Ryeom, S. (2005). Is oncogene addiction angiogenesis-dependent? Cold Spring Harb. Symp. Quant. Biol. *70*, 389–397.

Folkman, J., Heymach, J., and Kalluri, R. (2006). Tumor angiogenesis. In Cancer Medicine, D.W. Kufe, R.C. Bast, Jr., W.H. Hait, W.K. Hong, R.E. Pollack, R.R. Weichselbaum, J.F. Holland, and E. Frei, III, eds. (Ontario: BC Decker), pp. 157–191.

Gurtu, V., Kain, S.R., and Zhang, G. (1997). Fluorometric and colorimetric detection of caspase activity associated with apoptosis. Anal. Biochem. *251*, 98–102.

Hashizume, H., Baluk, P., Morikawa, S., McLean, J.W., Thurston, G., Roberge, S., Jain, R.K., and McDonald, D.M. (2000). Openings between defective endothelial cells explain tumor vessel leakiness. Am. J. Pathol. *156*, 1363–1380.

Hernandez, G.L., Volpert, O.V., Iniguez, M.A., Lorenzo, E., Martinez-Martinez, S., Grau, R., Fresno, M., and Redondo, J.M. (2001). Selective inhibition of vascular endothelial growth factor-mediated angiogenesis by cyclosporine A: Roles of the nuclear factor of activated T cells and cyclooxygenase 2. J. Exp. Med. *193*, 607–620.

Hesser, B.A., Liang, X.H., Camenisch, G., Yang, S., Lewin, D.A., Scheller, R., Ferrara, N., and Gerber, H.P. (2004). Down syndrome critical region protein 1 (DSCR1), a novel VEGF target gene that regulates expression of inflammatory markers on activated endothelial cells. Blood *104*, 149–158.

Hojo, M., Morimoto, T., Maluccio, M., Asano, T., Morimoto, K., Lagman, M., Shimbo, T., and Suthanthiran, M. (1999). Cyclosporine induces cancer progression by a cell-autonomous mechanism. Nature *397*, 530–534.

Iizuka, M., Abe, M., Shiiba, K., Sasaki, I., and Sato, Y. (2004). Down syndrome candidate region 1, a downstream target of VEGF, participates in endothelial cell migration and angiogenesis. J. Vasc. Res. *41*, 334–344.

Jauliac, S., Lopez-Rodriguez, C., Shaw, L.M., Brown, L.F., Rao, A., and Toker, A. (2002). The role of NFAT transcription factors in integrin-mediated carcinoma invasion. Nat. Cell Biol. *4*, 540–544.

Johnson, E.N., Lee, Y.M., Sander, T.L., Rabkin, E., Schoen, F.J., Kaushal, S., and Bischoff, J. (2003). NFATc1 mediates vascular endothelial growth factor-induced proliferation of human pulmonary valve endothelial cells. J. Biol. Chem. *278*, 1686–1692.

Kenyon, B.M., Browne, F., and D'Amato, R.J. (1997). Effects of thalidomide and related metabolites in a mouse corneal model of neovascularization. Exp. Eye Res. *64*, 971–978.

Liu, J., Farmer, J.D., Jr., Lane, W.S., Friedman, J., Weissman, I., and Schreiber, S.L. (1999). Calcineurin is a common target of cyclophilin-cyclosporin A and FKBP-FK506 complexes. Cell *66*, 807–815.

Minami, T., Horiuchi, K., Miura, M., Abid, M.R., Takabe, W., Noguchi, N., Kohro, T., Ge, X., Aburatani, H., Hamakubo, T., et al. (2004). Vascular endothelial growth factor- and thrombin-induced termination factor, Down syndrome critical region-1, attenuates endothelial cell proliferation and angiogenesis. J. Biol. Chem. *279*, 50537–50554.

Montrucchio, G., Lupia, E., Battaglia, E., Del Sorbo, L., Boccellino, M., Biancone, L., Emanuelli, G., and Camussi, G. (2000). Platelet-activating factor enhances vascular endothelial growth factor-induced endothelial cell motility and neoangiogenesis in a murine matrigel model. Arterioscler. Thromb. Vasc. Biol. *20*, 80–88.

O'Reilly, M.S., Boehm, T., Shing, Y., Fukai, N., Vasios, G., Lane, W.S., Flynn, E., Birkhead, J.R., Olsen, B.R., and Folkman, J. (1997). Endostatin: An endogenous inhibitor of angiogenesis and tumor growth. Cell *88*, 277–285.

Ozawa, M.G., Yao, V.J., Chanthery, Y.H., Troncoso, P., Uemura, A., Varner, A.S., Kasman, I.M., Pasqualini, R., Arap, W., and McDonald, D.M. (2005). Angiogenesis with pericyte abnormalities in a transgenic model of prostate carcinoma. Cancer *104*, 2104–2115.

Porter, A.G., and Janicke, R.U. (1999). Emerging roles of caspase-3 in apoptosis. Cell Death Differ. *6*, 299–306.

Qin, L., Zhao, D., Liu, X., Nagy, J.A., Hoang, M.V., Brown, L.F., Dvorak, H.F., and Zeng, H. (2006). Down syndrome candidate region 1 isoform 1 mediates angiogenesis through the calcineurin-NFAT pathway. Mol. Cancer Res. *4*, 811–820.

Ritter, O., Schuh, K., Brede, M., Rothlein, N., Burkard, N., Hein, L., and Neyses, L. (2003). AT2 receptor activation regulates myocardial eNOS expression via the calcineurin-NFAT pathway. FASEB J. *17*, 283–285.

Rossig, L., Li, H., Fisslthaler, B., Urbich, C., Fleming, I., Forstermann, U., Zeiher, A.M., and Dimmeler, S. (2002). Inhibitors of histone deacetylation downregulate the expression of endothelial nitric oxide synthase and

compromise endothelial cell function in vasorelaxation and angiogenesis. Circ. Res. *91*, 837–844.

Rothermel, B.A., Vega, R.B., and Williams, R.S. (2003). The role of modulatory calcineurin-interacting proteins in calcineurin signaling. Trends Cardiovasc. Med. *13*, 15–21.

Ryeom, S., Greenwald, R.J., Sharpe, A.H., and McKeon, F. (2003). The threshold pattern of calcineurin-dependent gene expression is altered by loss of the endogenous inhibitor calcipressin. Nat. Immunol. *4*, 874–881.

Vega, R.B., Rothermel, B.A., Weinheimer, C.J., Kovacs, A., Bassel-Duby, R., Williams, R.S., and Olson, E.N. (2002). Dual roles of modulatory calcineurin-interacting protein 1 in cardiac hypertrophy. Proc. Natl. Acad. Sci. USA *100*, 669–674.

Wang, H.G., Pathan, N., Ethell, I.M., Krajewski, S., Yamaguchi, Y., Shibasaki, F., McKeon, F., Bobo, T., Franke, T.F., and Reed, J.C. (1999). Ca2+-induced apoptosis through calcineurin dephosphorylation of BAD. Science *284*, 339–343.

Watanabe, K., Hasegawa, Y., Yamashita, H., Shimizu, K., Ding, Y., Abe, M., Ohta, H., Imagawa, K., Hojo, K., Maki, H., et al. (2004). Vasohibin as an endothelium-derived negative feedback regulator of angiogenesis. J. Clin. Invest. *114*, 898–907.

Yao, Y.G., and Duh, E.J. (2004). VEGF selectively induces Down syndrome critical region 1 gene expression in endothelial cells: A mechanism for feedback regulation of angiogenesis? Biochem. Biophys. Res. Commun. *321*, 648–656.